RESEARCH ARTICLE

Mathematical Model and Real-World Demonstration of Multi-Beam and Wide-Beam Reconfigurable Intelligent Surface

AMIRMASOOD BAGHERI[1], **MAHMOOD SAFAEI**[1], **ALI ARAGHI**[1], **(Member, IEEE)**,
S. M. MAHDI SHAHABI[1], **FAN WANG**[2], **MOHSEN KHALILY**[1], **(Senior Member, IEEE)**,
AND RAHIM TAFAZOLLI[1], **(Senior Member, IEEE)**

[1]Institute for Communication Systems (ICS), Home of the 5G and 6G Innovation Centre (5GIC and 6GIC), University of Surrey, GU2 7XH Guildford, U.K.
[2]Huawei Technologies Company Ltd., Shanghai 201206, China

Corresponding author: Mohsen Khalily (m.khalily@surrey.ac.uk)

ABSTRACT In this paper, a mathematical model is proposed to govern the phase distribution on a reconfigurable intelligent surface (RIS) for anomalously reflecting the beam towards the directions of interest. To this end, two operational modes are defined with respect to the reflected pattern. In the first mode, the RIS is configured to form multi-reflected beams toward the directions of interest capable of being controlled independently. The second mode is when the RIS provides a wide reflected beam. Regarding to each mode, a cost function is derived and then, in order to enhance the reflected pattern characteristics, a genetic algorithm (GA) is employed to the model as optimization method. To validate the practicality of the method, the proposed model is applied to a fabricated RIS to assess its performance in a real-world outdoor scenario. In the first mode, an asymmetric dual-beam reflected pattern is obtained and tested with tilt angles of $\theta_0 = 60°$ and $\theta_1 = 135°$. Furthermore, a wide-reflected beam is generated in the second mode with half-power beamwidth of $\theta_{HPBW} = 30°$ and tilt angle of $\theta_0 = 75°$. At both modes, the measured data are well aligned with the simulated results.

INDEX TERMS Reconfigurable intelligent surface (RIS), mathematical modeling, genetic algorithm (GA), beam forming, test-bed.

I. INTRODUCTION

Wireless communication is envisioned to be a fully connected world where there is a seamless connectivity for everyone and everything. The fifth-generation (5G) and the future sixth-generation (6G) communication networks would be required to meet such an ever-increasing demand for consistent connectivity. In this case, access to smart and efficient infrastructures for future generations of wireless networks would be inevitable.

In conventional cellular communications, controlling the adaptive features of the network are performed by either the base station (BS) or the user terminal equipments. This results in a propagation environment being unaware of various processes going through it. Accordingly, seamless connectivity,

The associate editor coordinating the review of this manuscript and approving it for publication was Shuai Liu.

especially in a highly congested environment, is one of the major challenges of the current mobile network operators [1].

In urban environments, large obstacles such as buildings, trees and walls along with the multi-path fading typically degrade the quality of service (QoS). To encounter these issues, while relay nodes might be employed as a solution, it leads to high power consumption of the whole network. In spite of several researches devoted to address aforementioned challenges, it still seems to remain as an open topic. Hence, a meaningful collaboration has been started between industrial and academic sections to bring some level of intelligence in combination of the passive radio propagation. One of the most promising technologies for solving aforementioned problem is the reconfigurable intelligent surface (RIS) being able to recycle the existing radio waves, enable NLoS communications and sense the environment [2]. RIS is capable of manipulating the impinging electromagnetic (EM) waves

and redirecting them to the desired angle while the power consumption would be relatively low compared to the relaying networks [3]. Therefore, to solve the coverage problem in current 5G and 6G wireless communications, RIS will play an important role.

RISs are typically composed of a metasurface sheet [4], [5] supported by a control unit. To be specific, the metasurface consists of a subgroup of periodic structures [6] embodied by repeating the so-called unit cells as the smallest pixel of the structure. Each unit cell usually possesses a conductive printed patch, referred to as scatterer, whose size is a small proportion of the operating wavelength. The interaction between such scatterers in a macroscopic scale makes a specific pattern to provide a desired phase distribution on the surface. By altering the phase distribution on the surface, the reflected wave from the metasurface sheet can be manipulated. In other words, each individual scatterer, or a cluster of them, can be characterised in such a way that the whole surface reconstructs the EM waves with desired properties. In order to reconfigure the response of the structure, each scatterer must be equipped with some components, e. g., PIN diode, varactor diode, MEMS and etc., which can be tuned electronically. The control unit is responsible for governing the performance of these tunable components. Having a control over the phase shift of each unit cell makes it theoretically possible to not only direct the reflected beam to the angle(s) of interest, but also shape it to a specific form.

Different approaches have been applied to regulate the phase distribution for generating multi-beam or contoured-beam EM-apertures [7], [8], [9], [10], [11]. In this respect, most of the presented methods are based on optimization algorithms [7], [8] or the superposition method [9], [11]. However, to the best of our knowledge, there have been no counterpart cases of research for RISs.

In order to have a more general solution, it is preferred to not only govern the beam's tilt angle, but also have control over the shape of the constructed beam. In case of RIS, this can provide us with an opportunity to incline the reflected beam towards the desired angle and consequently reshape it based on the coverage spot's requirements. For instance, the conventional base stations (BS) in cellular networks generate fan-beam radiation pattern to provide a relatively wide coverage footprint on the ground. This stems from the fact that users are more likely to be distributed over the azimuth plane in the body coordinates of the BS antenna and not over the elevation plane. The same scenario might be imagined for the case of RIS-aided cellular networks where the reflected beam is required to get a wider beamwidth in the azimuth plane to cover more users. Another probable scenario would be the case in which the impinging waves are required to be reflected toward more than one direction. In this article, we introduce an original mathematical model to shape the reflected beam in a RIS prototype.

Proposed approach, provides a phase distribution over RIS capable of shaping the reflection pattern as multi- or wide-beam patterns. Achieved patterns are aligned toward desired directions while in previous studies about RISs, only single beam steering scenarios have been considered [12], [13]. In a recent study [14], [15], a phase only method has been considered to provide multi-beam solution in order to address the coverage issue in practical scenarios. Considering single beam structures, same phase incremental steps regardless of the initial phase values can result in same far field patterns, if there was no variation in the amplitude response of unit-cell. Although the amplitude response variation of the unit-cells is inevitable and neglecting that degrades the parameters of reflection pattern beside the aperture efficiency of the structure. Accordingly, two operational modes are defined where in the first mode, the RIS is set to make a multi-beam reflection whereas the second mode would be defined when the RIS generates a wide reflected beam toward the direction of interest. In both cases, the mentioned amplitude behavior is considered.

Proposed cost functions for optimization technique are used in the genetic algorithm (GA) to find out the optimum suitable configurations of RIS. This optimization method has been previously used for beam steering in RISs which use PIN diodes and GA has shown its capabilities in providing real time solutions although other fast techniques are also applicable [16], [17]. In most of the previously phase assignation to RISs, only discrete phase responses are assumed for unit-cells [15], [17], [18]. In this regard, should be mentioned that neglecting the amplitude variation causes errors in shaping the desired reflection pattern [12], [18]. In this manuscript, the inter-relation of reflection coefficient and the imposed phase from the unit-cells is considered. This inter-relation is used for steering the beam efficiently in one hand, and on the other hand to improve the side lobe level of the overall beam. This feature is mostly neglected in previous studies [14], [15].

The rest of paper is organized as follows; in the next section, an expression is proposed to estimate the unit cell response. This forms the fundamental structure of our mathematical model. After that, the model is presented in details and then, in order to show its practicality, a dual-beam reflection pattern as an example of the first mode is obtained with independent control over the tilt angle of each beam. A tilted wide-beam reflection pattern is also generated using the model to validate the functionality of the second mode. Finally, we apply the presented model to a manufactured RIS which is our previous work [19] to assess the performance of the structure in a real-world scenario.

II. UNIT CELL'S ANALYTICAL EXPRESSION

The unit cell physical properties must be designed in a way that can properly manipulate the phase and amplitude of the reflected waves. Unit cells can be modeled by the equivalent circuit of Fig.1a, i. e., a RIS prototype [19] presented for the sake of illustration only, consisting a series of lumped RLC-elements. In general, by tuning the value of the capacitance C, the resonance frequency can be tailored in such a way to properly emulate the phase and amplitude response of the corresponding unit cells. The transmission line being terminated
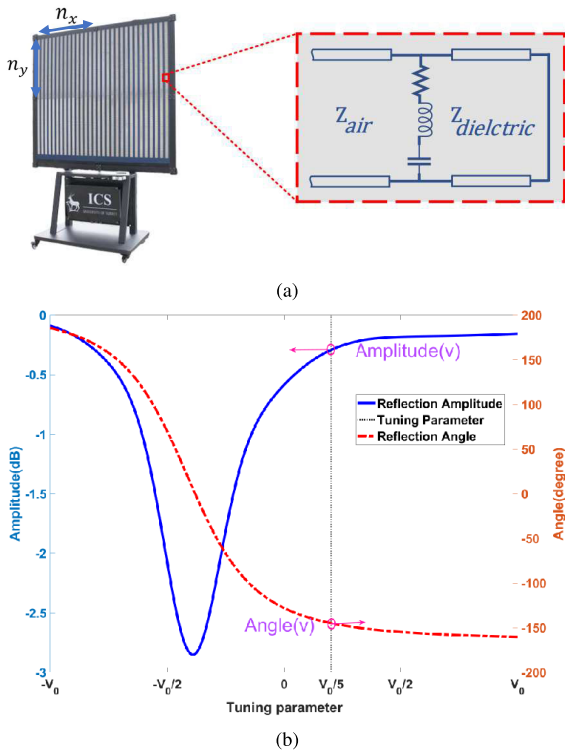
(a)

(b)

FIGURE 1. Unit cell attribute (a) Circuit model of the RIS unit cell. *m* and *n* represents the indices of unit cell. (b) unit cell response.

in a short circuit imitates the substrate characteristics. The circuit response can be an inspiration to propose a mathematical formula to express the unit cell performance. The obtained expression should be in line with a conventional resonating RLC circuit (Fig.1a). The tunability is usually obtained by applying a variable voltage (v) on each unit cell capable of being translated to reflection coefficient $\Gamma(v)$. In order to guarantee that the RIS have an appropriate performance, the following constraints should be met:

$$R\{\angle\Gamma(v)\} \approx 2\pi, \tag{1}$$

$$|\Gamma(v)| > -3\text{dB}, \tag{2}$$

where $R[\bullet]$ denotes the dynamic range of $\Gamma(v)$ while v sweeps over all its possible values. The amplitude of the reflecting waves from unit cells is proposed to be modeled as follows:

$$|\Gamma(v)| = 1 - (1 - A_0)\exp(-\frac{(v - v_0)^2}{2\sigma^2}), \tag{3}$$

where σ represents the standard deviation while A_0 and v_0 stands for the minimum reflection coefficient and its corresponding voltage, respectively. As shown in (3), the gaussian function might severely vary in the interval of $[v_0 - 2\sigma, v_0 + 2\sigma]$ being able to mimic the resonating trend of unit cells. For the sake of simplicity, v_0 can be assumed zero but σ is dependant on the unit cell geometry. Taking the second constraint into account, $\frac{A_0}{\sigma\sqrt{2\pi}}$ should be lower than $1 - \frac{1}{\sqrt{2}}$. The phase response of the unit cell versus tuning parameter

can be expressed as follows

$$\angle(\Gamma(v)) = \frac{a}{2}\tanh(v - v0) + b, \tag{4}$$

where a represents the obtainable phase range and b is the corresponding offset. In theory, a is preferred to be 2π which is not always achievable in practice [20]; It is shown that having a phase range of more than 300 degree is enough for beam steering [21].

Considering Fig.1b, $\angle(\Gamma(v))$ and $|\Gamma(v)|$ are two dependent functions so that altering $\angle(\Gamma(v))$ would change $|\Gamma(v)|$ as well. In some specific cases, this dependence can negatively affect the beamforming procedure [22] which would degrade the performance of reflected beam. This constraint affects the efficiency and also beam-width of the produced reflection pattern for any assignation to the RIS [18]. Additionally, it might seem that this limitation can only degrade the output of the design while in this manuscript is has been proposed and verified experimentally that a proper use of this response of unit-cells can also improve the overall features of the achievable output pattern. In this paper, we utilize this inter-related property between $\angle(\Gamma(v))$ and $|\Gamma(v)|$ to not only reshape the reflected beam but also reduce the SLL of the constructed beam. According to Fig.2, two states are defined (States 1& 2) where both are designed to concentrate the beam toward the angle of interest as they both possess similar phase progressions, i.e., $\Delta\phi_1$, $\Delta\phi_2$, $\Delta\phi_3$. As shown in Fig.2, mentioned different phase assignations while having same phase variation over RIS, does not provide same reflection pattern because of their respective amplitude variation. It should be mentioned that by changing the voltage and therefore assigning an amplitude(coefficient) to the local reflected beam, the phase response is also determined. Therefore, affects the efficiency and also beam-width of the produced reflection pattern for any assignation to the RIS. In this manuscript the respective amplitude/phase variation, has been used to improve the reflection pattern of RISs. Our proposed method is also verified experimentally and proposes that a proper use of this response from unit-cells can also improve the overall features of the achievable output pattern.

The main idea of this paper is to find counterpart zones on the phase curve where the phase progression remains almost constant as the amplitude characteristics are being optimized. To do so, we should first set the initial values of the phase shifts.

III. PROPOSED MATHEMATICAL MODEL

Taking the aforementioned concept into account, the required mathematical models are derived in this section to find the proper phase assignation over the aperture. We first explain the multi-beam operating mode with an example of generating a dual asymmetric reflected beams to showcase the practicality of the model. After that the second operating mode is described in details and a wide reflected beam is constructed.
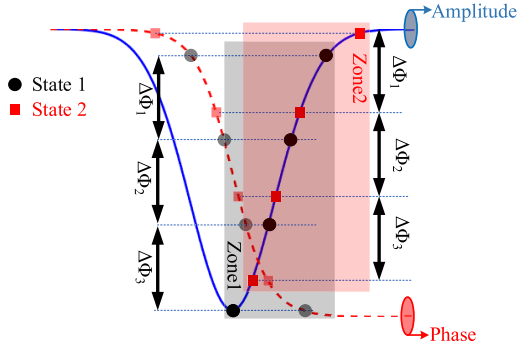
FIGURE 2. Conceptual description of the proposed optimization method.

A. FIRST OPERATING MODE: MULTI-BEAM FORMULATION

In several cases, it is desired to conduct the reflected wave from RISs in two, three or even more separate directions which are typically directed toward the blind spots. To this end, the following information should be known at the beginning of the procedure:

- Angles of blind spots with respect to the RIS.
- RIS gain toward each blind spot or sub-beam.
- Side-lobe level of the reflection pattern.

According to Eq.3 and Eq.4, by using the tuning parameter (v), an ordered pair of ($|\Gamma(v)|$, $\angle(\Gamma(v))$) can be determined. The applied voltage to the RIS makes a two dimensional matrix which can be reshaped into a one dimensional vector of $\vec{V} = \{v_1, v_2, \ldots, v_{N_u}\}$ with N_u denoting the total number of unit cells. Hence, the ordered pairs $\left(|\Gamma(\vec{V})|, \angle\Gamma(\vec{V})\right)$ are determined so that the reflection pattern of RIS ($G(\theta|\vec{V})$) can be calculated. Utilizing the reflection pattern, following attributes can be extracted

$$AT^m(\theta|\vec{V}) \triangleq \begin{cases} \hat{\theta}_0, \ldots, \hat{\theta}_{M-1} & \text{Estimated angles of} \\ & \text{maximum} \\ & \text{gain where } M \text{ is the number} \\ & \text{of beams,} \\ \hat{g}_0, \ldots, \hat{g}_{M-1} & \text{Estimated maximum gain at} \\ & \text{blind spot(s) direction(s),} \\ \hat{\delta g} & \text{SLL,} \end{cases} \tag{5}$$

in which that $\hat{\delta g}$ is the minimum value of the calculated vector $\vec{\delta g}(i) = \hat{g}_i - \hat{g}^{sl}$ for $i \in [0, 1, \ldots, M-1]$ while $\hat{g}^{sl}$ stands for the side-lobe gain. For a given $G(\theta|\vec{V})$ and by considering Eq. (5), other input parameters of the cost function (f^{mb}) are $\vec{\theta}$, $\vec{g}$, and δg which are expressed as

$$\begin{cases} \vec{\theta} = [\theta_0, \theta_1, \ldots, \theta_{M-1}], & \text{The desired tilt angles} \\ \vec{g} = [g_0, g_1, \ldots, g_{M-1}], & \text{Gain at the desired angles} \\ \delta g, & \text{Desired SLL} \end{cases} \tag{6}$$

In Eq. (5), θ varies from 0 to π covering the front hemisphere of the RIS. With $U(x_1, x_2)$ as a uniform random distribution between x_1 and x_2, initial configuration of unit cells in RIS is

assigned as follows

$$v_n \sim U(V_{min}, V_{max}) \quad \text{for all } n \in \{1, 2, 3, \ldots, N_u\}, \tag{7}$$

in which v_n is the random initial tuning parameter, i. e., the voltage of varactors, and V_{min} and V_{max} denote the minimum and maximum voltages respectively. With Γ_n as the reflection coefficient of nth unit cell, Eq. (3) and Eq. (4) result in

$$\angle\Gamma(\vec{V}) = \{\angle(\Gamma_1(v_1)), \angle(\Gamma_2(v_2)), \ldots, \angle(\Gamma_{N_u}(v_{N_u}))\} \tag{8}$$

$$|\Gamma(\vec{V})| = \{|\Gamma_1(v_1)|, |\Gamma_2(v_2)|, \ldots, |\Gamma_{N_u}(v_{N_u})|\} \tag{9}$$

where $|\Gamma(\vec{V})|$ and $\angle(\Gamma(\vec{V}))$ are the amplitude and phase vectors of RIS. The unit cell reflected pattern (P_u) can be defined as follows

$$P_u(G_0, \theta, \sigma_{HPBW}) = 10^{\left(\dfrac{G_0 \exp\left(-\dfrac{\theta^2}{2\sigma_{HPBW}^2}\right)}{20}\right)} \tag{10}$$

where σ_{HPBW} is the half power beam width (HPBW) and G_0 is the peak gain. To practically apply $\vec{V}$ to the RIS, it is required to use a digital logic such as digital to analogue converter (DAC). The corresponding quantized values are calculated by

$$\vec{V}_q = \left\{v_{DAC}(n)|(|v(n) - v_{DAC}(n)|) = \min(|v_n - V_{DAC}|)\right\}, \\ \text{for } n \in 1, 2, \ldots, N_u \tag{11}$$

in which $\vec{V}_q$ is the quantized voltage values of all unit cells, $v_{DAC}(n)$ is the nth quantized voltage, and V_{DAC} is a set of all possible voltages that DAC can provide in practice.

The far-field reflected pattern (c_{pat}) of the surface can be well approximated by

$$c_{pat}(\theta) = 20\log\Bigg(\sum_{m=1}^{N_u}\Big(P_u(G_0, \theta, \sigma_{HPBW}) \\ \times \exp(j\psi(\theta, \beta, \angle\Gamma_m(v_m) - \angle\Gamma_1(v_1), (m-1)d)) \\ \times |\Gamma_m(v_m)|\Big)\Bigg), \tag{12}$$

with β and d being the free-space wave-number and the size of unit cells, respectively. Also, ψ can be calculated by

$$\psi(\phi, \beta, \xi_j, d) = \beta d \cos\phi + \xi_j, \tag{13}$$

where ξ_j is the phase difference between the first and the j-th unit cell.

With reference to Eq. (12), a set of relative extremes and their corresponding angles can be extracted from the constructed pattern. Therefore, in order to generate M beams, the first $M+1$ relative extremes and their corresponding angles have been selected.

Regarding the defined parameters such as the angle of relative extrema, their corresponding gain and SLL, the cost function $f^{mb}(.)$ is proposed as follows:

$$f^{mb}(\vec{\theta}, \vec{g}, \delta g, G(\theta|\vec{V})) \\ = W_a(\vec{\theta} - \hat{\theta}_i)(\vec{\theta} - \hat{\theta}_i)^T$$
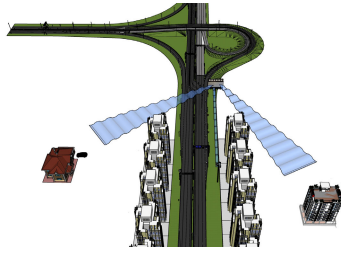
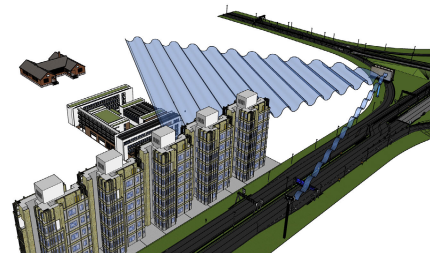**FIGURE 3.** Two beams asymmetric reflection ($\theta_1 \neq \theta_2$).
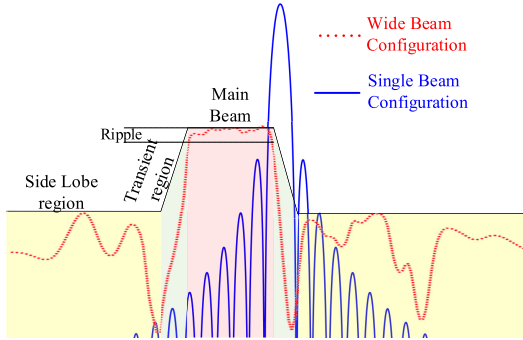

FIGURE 4. Beam specifications.

$$+ W_b(\vec{g} - \hat{g}_i)(\vec{g} - \hat{g}_i)^T + W_c(\delta g - \delta_{g_i})^2, \qquad (14)$$

in which W_a, W_b and W_c are weighing parameters to achieve the optimum result. In Eq. (14), Euclidean distance between the ideal goal and current situation are measured with respect to different attributes of the willing pattern. First, second, and third component in the right hand side of Eq. (14) implies the accuracy of the generated beam tilt angle, obtained gains and the achieved SLL, respectively. Second term in Eq. (14), provides the possibility of controlling the gain of the beams separately.

Fig. 3 illustrates a dual-beam reflection scenario toward the blind spots in an urban area.

B. SECOND OPERATING MODE: WIDE-BEAM FORMULATION

Beam specifications are presented in Fig. 4 for beam configurations of single and wide reflected patterns. As the single beam is transformed into the wide beam, the obtainable gain will be dropped with a ripple occurring at the main beam region. Thus, a transient region is defined between the main beam and side lobes, determining the sharpness of the constructed beam.

The maximum achievable beam width is directly affected by the required gain, i. e., the wider the beam the lower the gain. Driven by the fact that a beam is generally defined by its 3dB-HPBW, the maximum acceptable ripple level is set to be 3dB.

The wide-beam pattern can be expressed by θ_0 as the center angle of the main beam, $\delta\theta_0$ as the beamwidth, σ as the ripple, and δg as the SLL. These parameters should be extracted from $G(\theta|\vec{V})$ for any arrangement of $\vec{V}$. The corresponding attribute function for a wide beam configuration of RIS can

FIGURE 5. Wide-beam reflection scenario.

be written as follows

$$AT^w(\theta|\vec{V}) \triangleq \begin{cases} \hat{\theta}_0; & \text{Angle of maximum gain} \\ \hat{\sigma} = STD[G(\theta|\vec{V})]; & \theta \in [\hat{\theta}_0 - \frac{\delta\theta_0}{2}, \hat{\theta}_0 + \frac{\delta\theta_0}{2}] \\ \delta\hat{G}; & \bar{G} - G_{sl} \end{cases}$$
$$(15)$$

where $\bar{G}$ and G_{sl} denote the average gain of main beam and the maximum gain at the side lobe region, respectively. Also, $STD[G(\theta|\vec{V})]$ represents the standard deviation of $G(\theta|\vec{V})$ inside the main beam, i. e., $\theta \in [\hat{\theta}_0 - \frac{\delta\theta}{2}, \hat{\theta}_0 + \frac{\delta\theta}{2}]$). Input parameters of the cost function (f^{wb}) are $\theta_0, \delta\theta_0, \sigma, G(\theta|\vec{V})$. The front hemisphere of the RIS is divided into three sections referred to as main beam region, side-lobe region and transient region (see Fig. 4). the main beam region is defined as

$$B = [\theta_0 - \frac{\delta\theta_0}{2}, \theta_0 + \frac{\delta\theta_0}{2}] \qquad (16)$$

and side lobe region is written as follows

$$S = [0, \pi] - [\theta_0 - \frac{\delta\theta_0}{2} - \frac{\Delta}{2}, \theta_0 + \frac{\delta\theta_0}{2} + \frac{\Delta}{2}] \qquad (17)$$

where Δ is the width of transient region. In this way, the corresponding cost function (f^{wb}) is proposed as

$$f^{wb}(\theta_0, \delta\theta_0, \sigma, G(\theta|\vec{V}))$$
$$= W_a(\bar{G} - g_0)^2 + W_b(\hat{\sigma})^2$$
$$+ W_c(\hat{\theta}_0 - \theta_0)^2 + W_d(\delta g - \delta\hat{G})^2 \qquad (18)$$

which measures a weighed Euclidean distance between the current scenario and the desired state. A wide beam reflection scenario is shown in Fig. 5 for illustration purpose only.

In the following section, the proposed cost functions (f^{mu} and f^{wb}) are utilized in the optimization algorithm to achieve an optimum $\vec{V}$ that determines ordered pairs of assignation, i. e., phase/amplitude, for the unit cells.

IV. OPTIMIZATION METHOD FOR MULTI- AND WIDE-BEAM ALGORITHM

Genetic Algorithm (GA) is not a new concept in telecommunication research specifically in electromagnetic domain. One of the most trending research in electromagnetic field is designing array antennas and solving various complex multi-variable problems with GA. There have been several studies on GA-based algorithm for planner array synthesis and reducing the SLL of array antenna. There are some
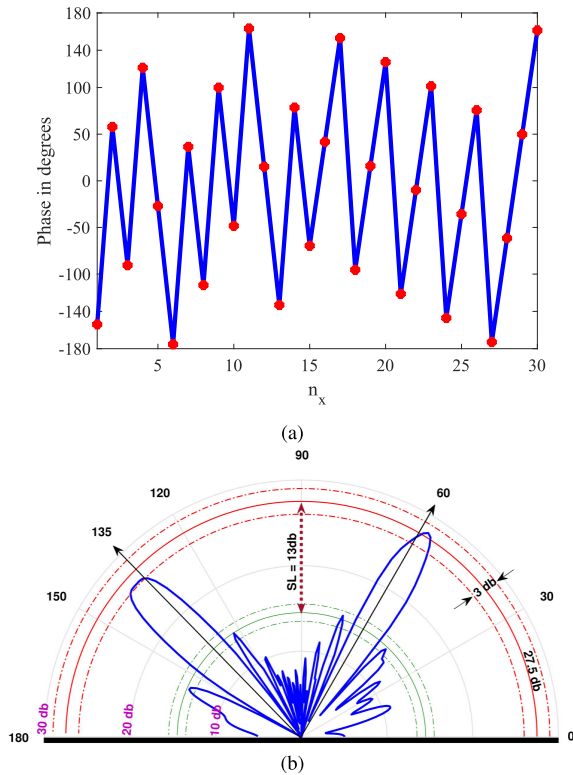
FIGURE 6. (a) The derived phase distribution over the aperture for a dual-beam scenario ($\theta_0 = 60$, $\theta_1 = 135$ and $\delta g = 13$dB) (b) The corresponding reflection pattern.

FIGURE 7. The derived phase distribution over the aperture for a wide beam scenario ($\theta_0 = 75$, $\delta\theta_0 = 30$ and $\delta g = 10$dB) (b) The corresponding reflection pattern.

extensive comparison study between GA and other optimization algorithms such as particle swarm to show which algorithms has Superior performance for complex synthesis [23]. Authors in [24] presented a comparison between amplitude-phase and phase-only synthesis in array antenna implies that that the amplitude-phase synthesis would outperforms the phase-only synthesis in terms of reducing side lobe levels. Shaping the beam pattern or beam-forming in array antenna is another issue researchers use hybrid methods to overcome.

GA concept is based on Darwin's theory which is a population-based algorithm. Each solution in GA corresponds to a gene and every parameter represent a chromosome and then combination of the multiple chromosomes makes a population. GA uses cost (fitness) function for any individual to evaluate their fitness. Randomness with a specific mechanism would be the best solution to improve and optimize a poor solution. Therefore, by comparing current state and the target using cost function, this operator can conduct the genes toward the best solution. One of the common issues in optimization algorithm is non-global optimum which means algorithm will stop to search for a better solution when it gets stuck into a local optimum. In order to avoid local optimum, GA selects poor solution with a probability as well. This mechanism can help GA to retrieve the good solution with other solutions if it is trapped in local optimum. GA is a stochastic algorithm. As a consequence, reliability in stochastic algorithms would be very crucial.
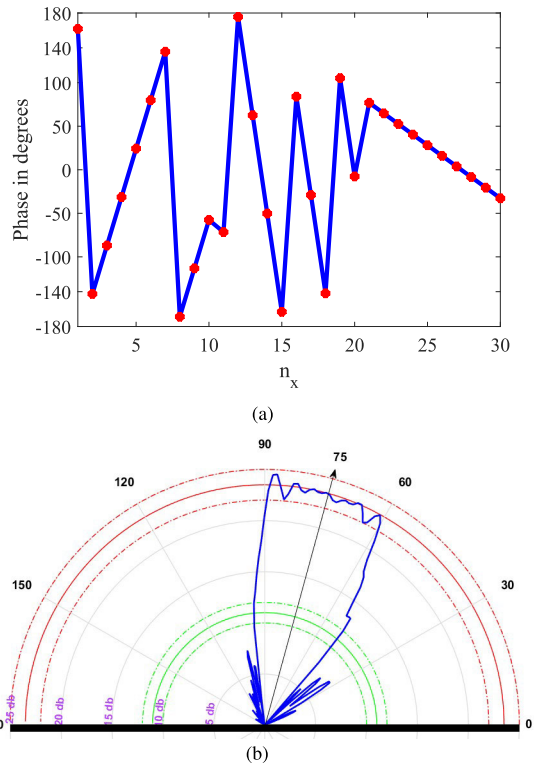
GA reliability and ability to estimate the optimum solution for a specific problem, are derived from maintaining the best solutions in each generation and using them to improve other solutions as well. Hence, the population turn into better solution generation by generation. GA benefits from two mechanisms called crossover and mutation. The crossover refers to swapping between two parents gen or gens and mutation is changing gens in each chromosome randomly. Mutation helps the diversity of each individual solution and increasing exploration behavior of the algorithm. Despite all of the good features that GA optimizer as an evolutionary technique can provide, it convergence speed might be slow in blind investigation for optimum parameters. In this regard, using look up tables can improve the speed of convergence. It relies on the similarity of the phase assignation of two states which their features like number of beams is same in one hand and on other hand the directions of their maximum reflection are close. Therefore, better initial population can improve the speed of convergence notably. Nevertheless, proposed cost functions can be used in any other optimization technique.

In this study the initial number of chromosomes is 1000. In addition, "mutation gaussian" and "crossover scattered" are selected as mutation algorithm and crossover algorithm, respectively.

By applying GA to Eq. (14) for the case of $\theta_1 = 60$, $\theta_2 = 135$, and $\delta g = 13$dB, the required phase distribution is derived as presented in Fig. 6a with the corresponding beam as shown in Fig. 6b. To obtain a wide beam reflection pattern with specifications of $\theta_0 = 75$, $\delta\theta_0 = 30$ and $\delta g = $

10dB, Eq. (18) is utilized in the GA which results in phase distribution of Fig 7a over the aperture with the constructed beam as shown in Fig. 7b.

V. RESULTS, DISCUSSIONS, AND PROOF OF CONCEPT

In this section, we explore how the proposed method can make a reflected beam out of the IRS. For this purpose, we first present the simulation results for two scenarios of two-asymmetric reflected beams and wide-reflected beam. The macroscopic response of the surface is controlled based on the properties of the developed unit cell which is explained in detail in [19]. The status of each unit cell is regulated by the proposed optimization algorithm. After that, we demonstrate a real-word performance of the designed IRS in a test-bed where the Tx is located 50 m away from the reflecting surface in an outdoor environment.

The demonstration replicates a scenario where the Rx receives no powerful signal from the Tx without employing the IRS in the environment. However, once the IRS is introduced to the scenario and is configured to reflect the beam to the angle of interest, a strong-enough signal would be captured by the Rx. This study shows that such entities can be used in 5G as well as future 6G networks to reshape the reflected beam in a desired form for ensuring an enhanced coverage footprint and a seamless connectivity to the users.

A. SIMULATING THE MACROSCOPIC RESPONSE OF THE SURFACE

The macroscopic response of the surface is governed by determining the microscopic performance of the unit cells. To this end, here we propose the following procedure.

- First, the properties of the reflection beam needs to be set as the input of the optimization algorithm, i. e., the relative reflection angles in case of multi-beam reflection and beam-width in case of wide-beam reflection.
- Then, with a Tx located far from the surface and by considering the angle of incidence (normal to the IRS aperture in our study), the phase distribution is calculated across each cluster of scatterers using the proposed algorithm.
- Subsequently, by considering this data, it is possible to map the calculated phase distribution to capacitances values by using the unit cell response plot shown in Fig. 4 of [19].
- Thereafter, the derived capacitances must be set in full-wave simulators such as Ansys HFSS or CST Studio SuiteB. by modifying the reactance value of a lumped element, attached to the scatterer for mimicing the effect of diode.
- Finally, the whole surface must be simulated, and the radar cross-section (RCS) pattern of the surface should be studied as the surface response for different scenarios of reflected beam.

Further to using CST Studio SuiteB. for simulating the structure, the outcome is presented in Fig. 8 (a) and (b) for two
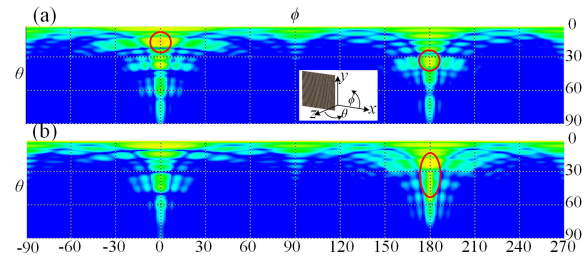

FIGURE 8. The simulated RCS of the surface. (a) two-asymmetric reflected beams, (b) wide reflected beam.
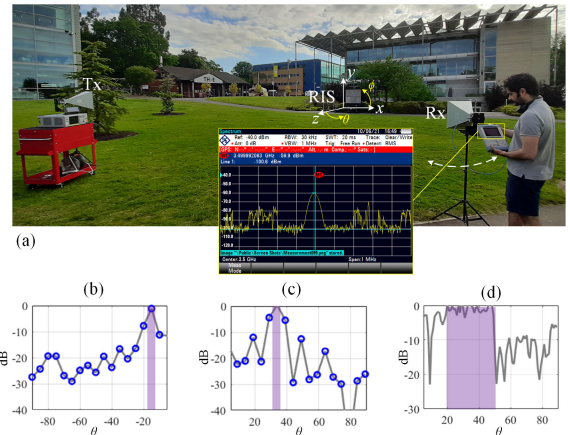

FIGURE 9. (a) Measurement campaign, (b) and (c) the dual-beam scenario, (d) the wide-beam scenario.

case studies of two-asymmetric reflected beams and wide reflected beam, respectively. These results demonstrate that the proposed algorithm can properly reshape the reflected beam toward the direction of interest.

To realize the designed RIS, it is required to convert the calculated capacitance values to specific voltage difference values across the SMV2202-040LF diodes by considering the respective characteristics of the diode on its datasheet. This data must be loaded as a look-up table in the control unit for each state of reflection. The corresponding values of biasing voltages would then be recalled in order to reconfigure the response of the whole surface. The control unit consists of an ARM microcontroller as the processing unit, a digital to analogue converter (DAC) for converting the look-up table, a set of operational amplifiers (Op-Amps) as the buffering system and a power supply unit.

B. TEST-BED SETUP AND EXPERIMENTAL RESULTS

In order to validate the proposed algorithm in a real-word scenario, an outdoor measurement campaign was conducted to examine the response of the developed IRS as shown in Fig. 9 (a).

For this purpose, two highly directive horn antennas with gain of more than 20 dBi was employed at both Tx and Rx sides. As a result of high directivity, the radiated waves toward directions other than the main beam are extremely weakened. This enables us to minimize the leakage from the side-lobes of the Tx to the Rx aperture by controlling the Tx power, so that the Rx received no detectable signal without

applying the RIS to the measurement campaign. Moreover, the use of a directional antenna would minimize the scattering effects from the surrounding environment to assure that the received signals are predominantly the reflected beams from the RIS and not from the potential multipath signals. The Tx antenna was fixed 50 m far from the RIS along its normal axis, 1.6 m above the ground to illuminate the surface at 3.5 GHz. The Rx antenna was connected to a spectrum analyzer to record the received signal at the operating frequency.

At the Rx side, in the RIS-free case, the received signal was nothing except the environmental noise. The designed RIS was then introduced into the scenario. After that, the IRS configures itself in order to direct the reflected waves toward the Rx at a specific angle of θ (see Fig. 9 (a)). As a consequence, a strong enough signal can be received at the Rx side. In order to derive the pattern of reflection, the received power was recorded at steps of 5° for a constant transmit power during the measurement procedure. The relative angle between the surface aperture and the Rx was changed from 10° to 90° while the radial distance between the surface and the Rx remained constant. The relative angle has been precisely tuned by using a laser meter along with the angle measurement tool. In the next stage, two scenarios were studied: first, the RIS was set to make two asymmetrical beams at $\theta_m = (-15°, 35°)$. The constructed reflection pattern is presented in Fig. 9 (b) and (c) in this case which shows that the surface is able to properly conduct the beam toward the direction of interest. It is worth noting that while the surface reconfigures itself corresponding to a specific direction of interest, the signal level at the receiver side is observed to be enhanced by more than 10 dB compared to the case when the surface is powered off. in second second scenario, the RIS was set to generate a widebeam reflection pattern with 3 dB beamwidth of 30° at the tilt angle of $\theta_m = 30°$. The corresponding measured data for this scenario is presented in Fig. 9 (d), showing the real-world practicality of the developed algorithm.

VI. CONCLUSION

RISs are introduced as a part of 5G and future 6G wireless networks. RISs play an crucial rule in potential technologies ensuring the coverage of wireless networks. In this paper, we proposed two mathematical models to form the reflected beam in two different operation modes. Utilizing the proposed mathematical models, proper phase distribution on the surface is achieved to amend the reflected beam into multi-beam and wide-beam as the first and second modes of the RIS respectively. In this paper, by considering the full response of unit-cells in RISs (amplitude and phase) beams are directed toward desired angles efficiently in one hand and on the other hand their side lobe level is also optimized using the local amplitude responses of the structure. For the sake of fully leveraging reflection pattern characteristic, a GA algorithm is applied to the proposed mathematical model. In order to evaluate the feasibility of the proposed construction, the devised model is expanded to a fabricated RIS.

REFERENCES

[1] B. Yang, X. Cao, C. Huang, C. Yuen, L. Qian, and M. D. Renzo, "Intelligent spectrum learning for wireless networks with reconfigurable intelligent surfaces," *IEEE Trans. Veh. Technol.*, vol. 70, no. 4, pp. 3920–3925, Apr. 2021.

[2] H. L. Zhang, B. Y. Di, L. Y. Song, and Z. Han, "Reconfigurable intelligent surfaces assisted communications with limited phase shifts: How many phase shifts are enough?" *IEEE Trans. Veh. Technol.*, vol. 69, no. 4, pp. 4498–4502, Apr. 2020.

[3] Y. Han, W. Tang, S. Jin, C. Wen, and X. Ma, "Large intelligent surface-assisted wireless communication exploiting statistical CSI," *IEEE Trans. Veh. Technol.*, vol. 68, no. 8, pp. 8238–8242, Jun. 2019.

[4] S. B. Glybovski, S. A. Tretyakov, P. A. Belov, Y. S. Kivshar, and C. R. Simovski, "Metasurfaces: From microwaves to visible," *Phys. Rep.*, vol. 634, pp. 1–72, Apr. 2016.

[5] M. Khalily, O. Yurduseven, T. J. Cui, Y. Hao, and G. V. Eleftheriades, "Engineered electromagnetic metasurfaces in wireless communications: Applications, research frontiers and future directions," *IEEE Commun. Mag.*, vol. 60, no. 10, pp. 88–94, Oct. 2022.

[6] A. Araghi, M. Khalily, P. Xiao, and R. Tafazolli, "Holographic-based leaky-wave structures: Transformation of guided waves to leaky waves," *IEEE Microw. Mag.*, vol. 22, no. 6, pp. 49–63, Jun. 2021.

[7] P. Nayeri, F. Yang, and A. Z. Elsherbeni, "Design and experiment of a single-feed quad-beam reflectarray antenna," *IEEE Trans. Antennas Propag.*, vol. 60, no. 2, pp. 1166–1171, Feb. 2012.

[8] P. Nayeri, F. Yang, and A. Z. Elsherbeni, "Design of single-feed reflectarray antennas with asymmetric multiple beams using the particle swarm optimization method," *IEEE Trans. Antennas Propag.*, vol. 61, no. 9, pp. 4598–4605, Sep. 2013.

[9] M. Karimipour and N. Komjani, "Holographic-inspired multibeam reflectarray with linear polarization," *IEEE Trans. Antennas Propag.*, vol. 66, no. 6, pp. 2870–2882, Jun. 2018.

[10] M. Karimipour and N. Komjani, "Realization of multiple concurrent beams with independent circular polarizations by holographic reflectarray," *IEEE Trans. Antennas Propag.*, vol. 66, no. 6, pp. 4627–4640, Sep. 2018.

[11] M. Karimipour, N. Komjani, and I. Aryanian, "Shaping electromagnetic waves with flexible and continuous control of the beam directions using holography and convolution theorem," *Sci. Rep.*, vol. 9, no. 1, pp. 1–13, Aug. 2019.

[12] H. Taghvaee, A. Cabellos-Aparicio, J. Georgiou, and S. Abadal, "Error analysis of programmable metasurfaces for beam steering," *IEEE J. Emerg. Sel. Topics Circuits Syst.*, vol. 10, no. 1, pp. 62–74, Mar. 2020.

[13] H. Taghvaee, S. Abadal, A. Pitilakis, O. Tsilipakos, A. C. Tasolamprou, C. Liaskos, M. Kafesaki, N. V. Kantartzis, A. Cabellos-Aparicio, and E. Alarcón, "Scalability analysis of programmable metasurfaces for beam steering," *IEEE Access*, vol. 8, pp. 105320–105334, 2020.

[14] H. Taghvaee, S. Terranova, N. M. Mohammed, and G. Gradoni, "Sustainable multi-user communication with reconfigurable intelligent surfaces in 5G wireless networks and beyond," in *Proc. 16th Eur. Conf. Antennas Propag. (EuCAP)*, Mar. 2022, pp. 1–5.

[15] A. B. Masood, V. Vassiliou, A. Pitsillides, C. Liaskos, and M. Lestas, "Multivariable extremum seeking controllers for multi-beam steering using reconfigurable metasurfaces," in *Proc. IEEE Globecom Workshops (GC Wkshps)*, Dec. 2022, pp. 49–54.

[16] C. Rizza, V. Loscrí, and M. O. Parchin, "Real-time beam steering in mmWave with reconfigurable intelligent meta-surfaces," in *Proc. IEEE Global Commun. Conf. (GLOBECOM)*, Dec. 2021, pp. 1–6.

[17] X. Meng, M. Nekovee, and D. Wu, "The design and analysis of electronically reconfigurable liquid crystal-based reflectarray metasurface for 6G beamforming, beamsteering, and beamsplitting," *IEEE Access*, vol. 9, pp. 155564–155575, 2021.

[18] H. Rajabalipanah, A. Abdolali, J. Shabanpour, A. Momeni, and A. Cheldavi, "Asymmetric spatial power dividers using phase–amplitude metasurfaces driven by Huygens principle," *ACS Omega*, vol. 4, no. 10, pp. 14340–14352, 2019.

[19] A. Araghi, M. Khalily, M. Safaei, A. Bagheri, V. Singh, F. Wang, and R. Tafazolli, "Reconfigurable intelligent surface (RIS) in the sub-6 GHz band: Design, implementation, and real-world demonstration," *IEEE Access*, vol. 10, pp. 2646–2655, 2022.

[20] M. Jung, W. Saad, M. Debbah, and C. S. Hong, "On the optimality of reconfigurable intelligent surfaces (RISs): Passive beamforming, modulation, and resource allocation," *IEEE Trans. Wireless Commun.*, vol. 20, no. 7, pp. 4347–4363, Jul. 2021.

[21] P. Nayeri, F. Yang, and A. Z. Elsherbeni, *Reflectarray Antennas: Theory, Designs, and Applications*. Hoboken, NJ, USA: Wiley, 2018.

[22] A. Araghi, M. Khalily, P. Xiao, R. Tafazolli, and D. R. Jackson, "Long slot mmWave low-SLL periodic-modulated leaky-wave antenna based on empty SIW," *IEEE Trans. Antennas Propag.*, vol. 70, no. 3, pp. 1857–1868, Mar. 2022.

[23] D. W. Boeringer and D. H. Werner, "Particle swarm optimization versus genetic algorithms for phased array synthesis," *IEEE Trans. Antennas Propag.*, vol. 52, no. 3, pp. 771–779, Mar. 2004. [Online]. Available: http://ieeexplore.ieee.org/document/1288473/

[24] G. K. Mahanti, A. Chakraborty, and S. Das, "Phase-only and amplitude-phase only synthesis of dual-beam pattern linear antenna arrays using floating-point genetic algorithms," *Prog. Electromagn. Res.*, vol. 68, pp. 247–259, 2007.

AMIRMASOOD BAGHERI was born in Tehran, Iran, in December 1991. He received the B.Sc., M.Sc., and Ph.D. degrees from the Faculty of Electrical Engineering, Sharif University of Technology, Tehran, in 2013, 2015, and 2021, respectively. He is currently a Research Fellow with the Institute for Communication Systems (ICS), Home of the 5G and 6G Innovation Centre (5GIC and 6GIC), University of Surrey, Guildford, U.K. He is a Research Assistant with the National Physical Laboratory (NPL), London, U.K. His research interests include reconfigurable devices at microwave and mmW regimes besides their applications in 5G and 6G communication generations.

MAHMOOD SAFAEI received the Ph.D. degree in computer science from the Faculty of Engineering, University of Technology Malaysia. He is currently a Research Fellow with the Institute for Communication Systems (ICS), Home of the 5G and 6G Innovation Center (5GIC and 6GIC), University of Surrey, Guildford, U.K. His research interests include embedded systems, the Internet of Things, wireless sensor networks, cyber security, smart grid, and security in the IoT devices.

ALI ARAGHI (Member, IEEE) received the M.Sc. degree in telecommunication-wave engineering from Shahed University, Tehran, Iran, in 2012, and the Ph.D. degree from the Institute for Communication Systems (ICS), Home of the 5G and 6G Innovation Center (5GIC and 6GIC), University of Surrey, Guildford, U.K., in 2023. He worked at the Iran Telecommunication Research Center (ITRC) as a Research Assistant on antennas and propagation, from 2012 to October 2018. He is currently a Research Assistant with the Sensors Systems and Circuits Group, Department of Electronic and Electrical Engineering, University College London (UCL), London, U.K. His main research interests include leaky-wave structures, holography theory, metasurfaces, intelligence-reflecting surfaces, and the theory of characteristic modes. He was endorsed as "Global Talent" by the Royal Academy of Engineering, U.K., in 2022. He was also a recipient of the Industrial Advisory Board "Departmental Prize for Excellence in Research" from the Faculty of Engineering and Physical Sciences (FEPS), University of Surrey, in 2022.

S. M. MAHDI SHAHABI received the B.Sc. degree in electrical engineering from the University of Tehran, Iran, in 2010, the M.Sc. degree in electrical engineering from the Amirkabir University of Technology, Tehran, in 2013, and the Ph.D. degree in electrical engineering from the K. N. Toosi University of Technology, Tehran, in 2019. He was a Postdoctoral Research Associate in wireless communications at the Centre for Telecommunications Research (CTR), King's College London (KCL), London, U.K., from 2020 to 2021. He is currently a Research Fellow with the 6G Innovation Centre (6GIC), University of Surrey, Guildford, U.K., mainly focusing on 5G and 6G communications. His research interests include wireless communications and signal processing, with a particular focus on reconfigurable intelligent surfaces (RIS), MIMO and massive MIMO systems, optimization theory, and artificial intelligence.

FAN WANG received the B.S. and Ph.D. degrees in electronic engineering from Zhejiang University, Hangzhou, China. He joined Huawei Technologies Company Ltd., Shanghai, China, in 2008. From 2015 to 2016, he was with Huawei Technologies Sweden AB, Kista, Sweden. From 2019 to 2021, he was with Huawei Technologies Company Ltd., Reading, U.K. He has contributed to 3G/4G/5G physical layer standardization work and held numerous patents. His current research interests include B5G/6G wireless communication and massive machine-type communication.

MOHSEN KHALILY (Senior Member, IEEE) is currently a Senior Lecturer (Associate Professor) in antennas and propagation and the Head of the Surface Electromagnetics Laboratory, Institute for Communication Systems, University of Surrey, U.K. He has published four book chapters and almost 200 academic papers in international peer-reviewed journals and conference proceedings. He has been the principal investigator on research grants totaling in excess of £1.6 million in the field of surface electromagnetic. His research interests include surface electromagnetics, electromagnetic-engineered metasurfaces, phased arrays, THz meta devices, and mmWave and THz propagation. He is a Delegate Member of the ETSI Industrial Specification Group on Reconfigurable Intelligent Surfaces and a fellow of the U.K. Higher Education Academy. He serves as an Associate Editor for the IEEE ANTENNAS AND WIRELESS PROPAGATION LETTERS, *Scientific Reports*, and IEEE ACCESS.

RAHIM TAFAZOLLI (Senior Member, IEEE) has been a Professor of mobile and satellite communications, since April 2000. He has also been the Director of the Institute for Communication Systems (ICS), since January 2010, and the Founder and the Director of the 5G Innovation Centre, University of Surrey, U.K. He has more than 25 years of experience in digital communications research and teaching. He has authored or coauthored more than 500 research publications. He is a co-inventor on more than 30 granted patents, all in the field of digital communications. He is regularly invited to deliver keynote talks and distinguished lectures to international conferences and workshops and many governments for advice on 5G technologies. He was an Advisor to the Mayor of London in regard to the London Infrastructure Investment 2050 Plan, from May 2014 to June 2014. He has given many interviews to international media in the form of television, radio interviews, and articles in the international press. In 2011, he was appointed as a fellow of the Wireless World Research Forum (WWRF) in recognition of his personal contributions to the wireless world and the heading of one of Europe's leading research groups.

• • •